Energy Proceedings
Vol 52, 2025
ISSN 2004-2965

Assessment of Solar Irradiance Based on Sky Image Capturing and Near-ground Meteorology Measurements#

Shuhao Wang[1], Jinqing Peng[1,2*]

1 College of Civil Engineering, Hunan University, Changsha, 410082, China
2 Key Laboratory of Building Safety and Energy Efficiency of Ministry of Education, Hunan University, Changsha, 410082, China
(*Corresponding Author: jqpeng@hnu.edu.cn)

ABSTRACT

Solar PV generation makes a great contribution to promoting renewable energy development. However, the unpredictable cloud cover makes PV generation to become unstable. This study developed a novel method to evaluate the cloud cover with sky images and subaerial meteorology parameters. The improved sun tracking model, RBR threshold model were combined to upgrade the simulation precision of cloud cover in the sky. Validation shows the developed method performs well under the different sky conditions. Furthermore, this study investigated the impact of the sky state and the near-ground visibility on solar irradiance. This study provides a thorough method for evaluating the cloud cover, which may instruct the industry to deal with instable solar irradiance under different sky states and prompt the solar PV application.

Keywords: Cloud cover; Sky state evaluation; Solar irradiance; Visibility measurements

NONMENCLATURE

Abbreviations	
DNI	Direct normal irradiance
DHI	Diffuse horizontal irradiance
GHI	Global horizontal irradiance
PV	Photovoltaic
RBR	The pixel ratio of red channel and blued channel
Symbols	
X	X axis of sky image
Y	Y axis of sky image
L	Image dimension
Δ	Deviation
α	Altitude angle
β	Azimuth
n	Number
θ	Altitude angle of the sun
Superscript and Subscript	
′	Simulated
sun	The sun
re	Revised

1. INTRODUCTION

Photovoltaic (PV) generation is a kind of fundamental technology to promote the renewable energy development. The PV installed capacity has been gradually increased in recent years, reflecting a decent prospective progress [1]. Nevertheless, the intermittent solar irradiance can make PV cells generate unstably, which impedes the development of PV technology. The sky state and the near-ground visibility become the main influence factors which cause the solar irradiance arriving on the surface intermittently [2]. Therefore, it is meaningful to assess the impacts of the sky state and the near-ground visibility on solar irradiance for PV industry.

An effective method to analyze the relationship between sky state and solar irradiance is to capture the sky image via camera. Alessandro et al. [3] identified the sky illuminance and sun position through sky imaging. Martinez Lopez et al. [4] achieved the short-term irradiance prediction by modeling the cloudiness monitoring based on the sky image analysis. However, a sufficient consideration of lens distortion was missed while processing the sky state evaluation. Besides, the literature few concerns the near-ground meteorology which can also make an evident influence on solar irradiance, especially visibility.

This paper conducted an assessment for property of solar irradiance based on combining the sky state with the near-ground meteorology. The sky state is obtained by proposing a method on considering lens distortion. Then a property analysis of the solar irradiance under different sky state and visibility conditions was conducted. This paper may contribute to dealing with instable photovoltaic output under different sky states and near-ground visibility for the PV industry.

This is a paper for the 16th International Conference on Applied Energy (ICAE2024), Sep. 1-5, 2024, Niigata, Japan.

2. METHODOLOGY

2.1 Measurements and setups

The field measurement is sited in Changsha, China (latitude 28°10' north, longitude 112°56' east). The direct normal irradiance (DNI), the diffuse horizontal irradiance (DHI), and the global horizontal irradiance (GHI) were acquired by pyranometers. Meanwhile, this paper captured the sky information by the all-sky imager and measured the near-ground meteorology parameters including air temperature, humidity, pressure and visibility. The all instruments above were sampled once per minute synchronously. The samples was eliminated when the GHI is less than 20 W/m^2 to avoid the dead zone of instrument and the unnatural solar irradiance.

2.2 Sky state evaluation

The sun and the cloud are the two essential elements in the sky image. It is crucial for determining sky state to acquire the sun exposure and the cloud cover.

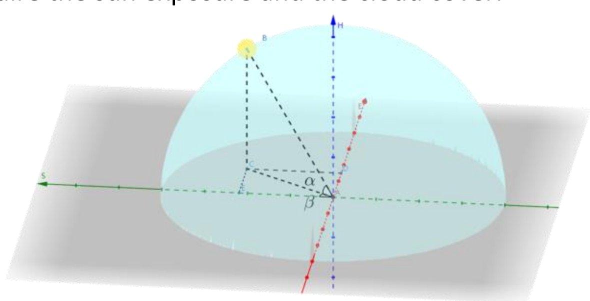

Fig. 1 Basic sun position model

The sun exposure describes the level of the sun covered by the cloud. As shown in **Fig. 1**, the basic method to track the sun position in the sky image depends on the altitude angle and the azimuth of the sun, which is expressed as follows [5]:

$$\begin{bmatrix} X'_{sun} \\ Y'_{sun} \end{bmatrix} = \begin{bmatrix} 1 & -\cos\alpha\sin\beta \\ 1 & +\cos\alpha\cos\beta \end{bmatrix} \begin{bmatrix} L \\ L \end{bmatrix} \tag{1}$$

Where X'_{sun} and Y'_{sun} represent the simulated sun position, $\begin{bmatrix} L \\ L \end{bmatrix}$ is the image dimension matrix, α and β represent the altitude angle and the azimuth of the sun, respectively. However, this method ignores the lens distortion especially when the sun approaches to the edge of sky. A significant deviation will appear between the sun position simulated by the method and the sun position captured in the image. This paper used the grayscale method to capture the sun position in the image, calculating the difference between the simulated sun position and the captured sun position, which is shown as follows:

$$\begin{bmatrix} \Delta X_{sun} \\ \Delta Y_{sun} \end{bmatrix} = \begin{bmatrix} X'_{sun} - X_{sun} \\ Y'_{sun} - Y_{sun} \end{bmatrix} \tag{2}$$

Where X_{sun} and Y_{sun} represent the captured sun position by sky imaging, ΔX_{sun} and ΔY_{sun} represent the deviation of the sun position. This paper analyzed the daily variation feature of the deviation of the sun position and established an empirical expression by using the hour angle. Finally, combining the deviation estimated by the empirical expression with the simulated sun position, the revised sun position considering the lens distortion can be obtained, which is expressed as follows:

$$\begin{bmatrix} X_{sun,re} \\ Y_{sun,re} \end{bmatrix} = \begin{bmatrix} X_{sun} + \Delta X'_{sun} \\ Y_{sun} + \Delta Y'_{sun} \end{bmatrix} \tag{3}$$

Where $X_{sun,re}$ and $Y_{sun,re}$ represent the revised sun position, $\Delta X'_{sun}$ and $\Delta Y'_{sun}$ represent the deviation estimated by the empirical expression. According to the literature, the pixel value of the sun in the image commonly exceeds 150 [6]. This paper counted the number of pixels over 150 around the revised sun position to calculate the sun exposure, which is shown as follows:

$$Sun\ Exposure = \frac{n(Pixel \geq 150)}{n(Sun\ Aera)} \tag{4}$$

There is the more complete sun if the sun exposure is closer to 1.

The cloud cover represents the state of the sky obscured by clouds. Researchers commonly distinguish clouds and the sky dome by comparing the pixels value of red channel and blue channel [7]. After deleting sun pixels, this paper investigates the RBR ratio of the image according to the follows [8]:

$$RBR = \frac{P_R}{P_B} \Big/ \left(\frac{P_R}{P_B}\right)_{max} \tag{5}$$

Where P_R and P_B represent the pixel value of red channel and blue channel, $\left(\frac{P_R}{P_B}\right)_{max}$ is the maximum value of $\frac{P_R}{P_B}$ for the image. The RBR of clouds is commonly larger than 0.4, which becomes a support of identifying clouds [9]. Therefore, the cloud cover can be estimated as follows:

$$Cloud\ Cover = \frac{n(RB \geq 0.4)}{n(Sky\ Aera)} \tag{6}$$

When the cloud cover is closer to 1, the cloudiness covering the sky will be larger.

2.3 Near-ground evaluation

The visibility near the ground also has a great impact on solar irradiance. The main reason lies on that the contamination particles close to the surface can induce the scattering effect, attenuating the solar irradiance arriving on the ground. According to Dogniaux's model, visibility can describe the near-ground turbidity which reflects contamination particles [10]. However, the visibility sensor may produce a deviation when the visibility is less than 3 km according to the instrument principle. Therefore, this paper eliminates the samples with the visibility below 3 km.

3. RESULTS AND DISCUSSION

3.1. Validation for sky states evaluation

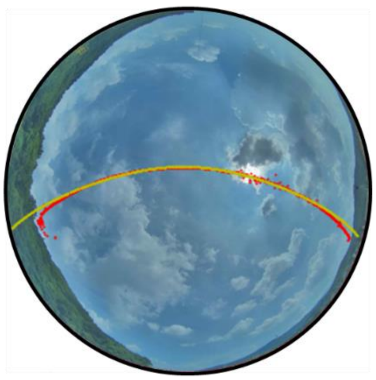

Fig. 2 Sun position tracking

It is of great importance for determining the sky state to obtain a precise sun position. Due to constrained sun pixels in sky images, the sky state might be misjudged by the slight sun position deviation. This paper investigated the sun position during a day according to **Eq. (3)** and compared the result with the image capturing. **Fig. 2** shows the revised sun position in yellow and the captured sun position in red for a day. Overall, the revised position agrees well with the captured sun position, which reveals the excellent performance of the proposed method on obtaining the sun position. A slight deviation between them happened at the sunrise or sunset. However, the solar irradiance at that moment commonly stays at a low level, which hardly has the contribution to solar energy application. Noticeably, when the sun is obscured by clouds, the grayscale method will misjudge the maximum gray value as the sun position. As a result, the captured sun position formed a discontinuous curve with some discrete points. Based on the revised sun position, the sun exposure was investigated further according to **Eq. (4)**. Due to the constrained sun pixels, the sun often stayed entirely exposed or entirely obscured. Over 90% sun exposure frequently equals to 1 or 0. As a result, the sky images were divided into two categories: the sun exposed (sun exposure=1) and the sun covered (sun exposure=0).

This paper simulated the cloud cover under different states of the sky obscured by clouds. **Fig. 3** shows the simulation results of cloud cover under two categories. The sun pixels were deducted from the sky dome before calculating the cloud cover. When the sun is totally exposed, the RBR method can distinguish the sky and clouds well. Only a few clouds close to the horizon failed to be identified due to the dark brightness. Another minor dark cloud was not identified because of its color extremely similar to the sky. When the sun is totally covered, most of clouds area was greatly identified by the RBR method as well. However, a minor part of sky close to the horizon was wrongly regarded as clouds. The city contaminants will induce the scattering effect, making the sky close to the horizon brighten especially when the sun was covered. Therefore, the scattering light may be misjudged as clouds.

3.2. Impacts of sky state and near-ground meteorology on solar irradiance

For assessing the impact of sky state and near-ground meteorology on solar irradiance, the variation of GHI

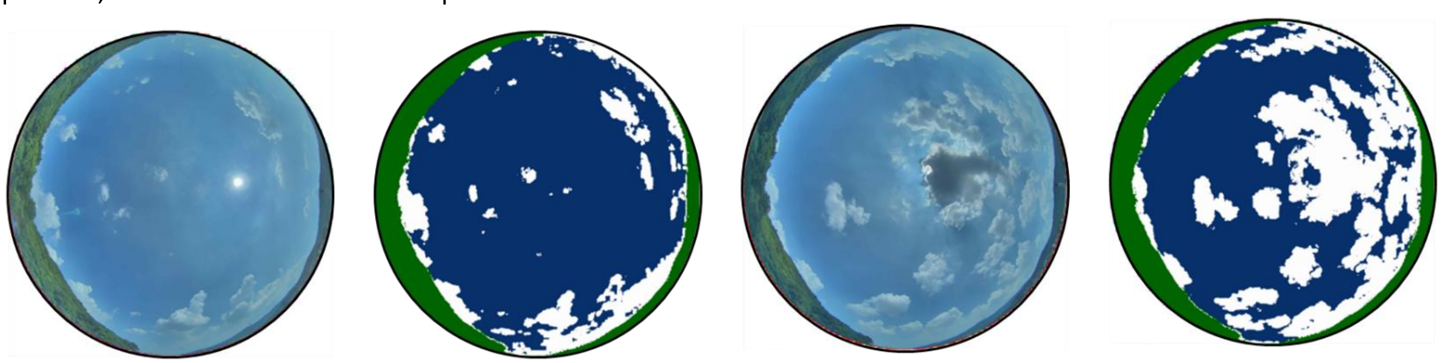

(a) (b) (c) (d)

Fig. 3 (a) Sky image when sun exposure is 1; (b) cloud simulation when sun exposure is 1; (c) sky image when sun exposure is 0; (d) cloud simulation when sun exposure is 0.

against the cloud cover and visibility was analyzed. This paper calculated the cloud cover of all the sky images captured in the measurement period. Then the samples with disqualified GHI and visibility were eliminated for the instrument limitation. **Fig. 4** manifests the GHI distribution against the cloud cover and visibility. Obviously, the GHI is overall increased with the rising visibility. However, the cloud cover kept around 0.5 when the GHI approach to the peak, instead near 0. The reason may be explained that the situation that the cloud cover equals 0 commonly occurs in the morning or evening in Changsha. When the GHI stays a large value, the water vapor will be produced favorably. As a result, cloud will follow properly at the high GHI level.

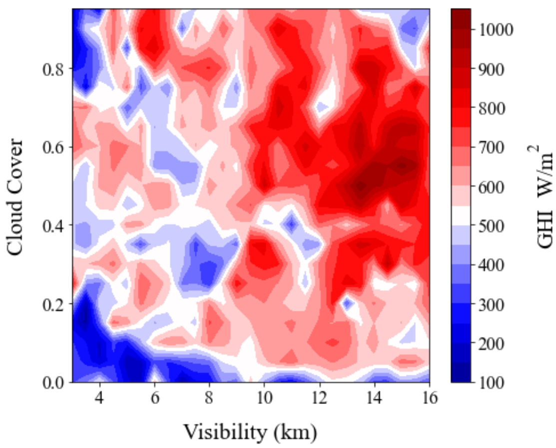

Fig. 4 GHI distribution

It is also vital to analyze the component variation of the GHI for applying solar energy appropriately. The DNI component has a great amount of irradiance but get influenced by the incident angle while applying to the façade. The DHI component has a little amount of irradiance but it is independent of façade orientation. In this paper, R_{DD} was defined as the ratio of the product of DNI and $\sin\theta$ to DHI, to reflect the dominant factor in the GHI. **Fig. 5** displays the R_{DD} distribution against different sky states and near-ground meteorology situation. Apparently, the RDD is positively correlated to the visibility and negatively correlated to the cloud cover. For one thing, a great visibility value indicates a few contaminants in the air, which only generates the slight scattering effect. However, due to the effect of solar altitude mentioned above, the DNI component decreases after the visibility exceeds 15 km. For the other, a large cloud cover suggests that most DNI may be blocked and scattered by clouds, which attenuates the DNI and increases the DHI arriving on the surface. Nevertheless, the DNI is still far larger than the DHI unless the sun is totally covered.

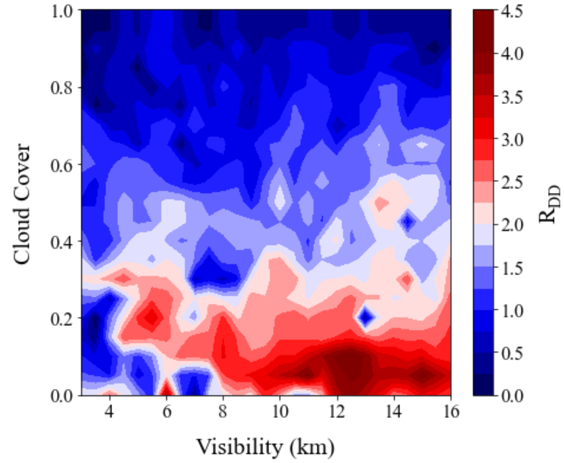

Fig. 5 R_{DD} distribution

4. CONCLUSIONS

This paper assessed the property of solar irradiance by obtaining the sky state and near-ground meteorology. An improved method based on the sky imaging was developed to evaluate the sky state. Result shows that the sun position and the cloud cover can be identified well under different sky states. Furthermore, this paper investigated the impact of sky state and near-ground meteorology on solar irradiance. The GHI distribution exists a peak as the cloud cover diminishes, and the R_{DD} distribution also exists a peak as the visibility increases. This paper may instruct the industry to deal with instable solar irradiance under different sky types and prompt the solar PV application.

ACKNOWLEDGEMENT

The study was supported by the National Natural Science Foundation of China [grant numbers 52278104], and the Science and Technology Innovation Program of Hunan Province [grant number 2023RC1042].

REFERENCE

[1] Liang H, Shen J, Yip HL, et al. Unleashing the green potential: Assessing Hong Kong's building solar PV capacity. Applied Energy 369 (2024) 123567.

[2] Gueymard CA. Visibility, aerosol conditions, and irradiance attenuation close to the ground—Comments on "Solar radiation attenuation in solar tower plants" by J. Ballestrin and A. Marzo, Solar Energy (2012)[J]. Solar Energy, 2012, 86(5):1667-1668. DOI:10.1016/j.solener.2011.12.027.

[3] Niccolai A, Nespoli A. Sun Position Identification in Sky Images for Nowcasting Application[J]. IEEE, 2020. DOI:10.1109/EEEIC/ICPSEurope49358.2020.9160490.

[4] Martinez Lopez VA, Gijs van U, Pim J.F. D, et al. Using sky-classification to improve the short-term prediction of

irradiance with sky images and convolutional neural networks. Solar Energy 269 (2024) 112320.
[5] Jensen AR, Sifnaios I, Anderson K. *twoaxistracking* – a python package for simulating self-shading of two-axis tracking solar collectors. MethodsX 9 (2022) 101876.
[6] Zuo H-M, Qiu J, Jia Y-H, et al. Ten-minute prediction of solar irradiance based on cloud detection and a long short-term memory (LSTM) model. Energy Reports 8 (2022) 5146–5157.
[7] Shields J E, Karr M E, Burden A R, et al. Research toward Multi-site Characterization of Sky Obscuration by Clouds [J]. 2009.
[8] Chow C W, Urquhart B, Lave M, et al. Intra-hour forecasting with a total sky imager at the UC San Diego solar energy testbed[J]. Solar Energy, 2011, 85(11):2881-2893. DOI: 10.1016/j.solener.2011.08.025.
[9] Bernecker D, Riess C, Angelopoulou E, et al. Continuous short-term irradiance forecasts using sky images[J]. Solar Energy, 2014, 110(dec.):303 – 315. DOI:10.1016/j.solener.2014.09.005.
[10] Dogniaux R. Distribution of solar radiation in Saudi Arabia[J]. Heliotechnique and Development, Volume 1, 1976.